Modern Physics Letters B
Vol. 33, No. 21 (2019) 1950241 (8 pages)

DOI: 10.1142/S0217984919502415

Influences of second-order and third-order dispersion on spectral properties of mid-infrared wavelength conversion in silicon nitride waveguides

Peng Xie[*,†,‡,§,**], Jiarui Liu[¶], Yu Wen[‖], Zishen Wan[‡] and Yishan Wang[*,§]

[*] *State Key Laboratory of Transient Optics and Photonics, Xi'an Institute of Optics and Precision Mechanics, Chinese Academy of Sciences, Xi'an 710119, China*
[†] *Department of Mechanical Engineering, Massachusetts Institute of Technology, Cambridge 02139, USA*
[‡] *School of Engineering and Applied Sciences, Harvard University, Cambridge 02138, USA*
[§] *University of Chinese Academy of Sciences, Beijing 100049, China*
[¶] *Sun Yat-Sen University, Guangzhou 510000, China*
[‖] *National University of Defence Technology, Changsha 410073, China*
[**] *pengxie@mit.edu*

Received 8 April 2019
Revised 16 April 2019
Accepted 8 May 2019
Published 17 July 2019

The influences of second-order dispersion (SOD) and third-order dispersion (TOD) on spectral properties of wavelength conversion based on FWM at mid-infrared region (mid-IR) are theoretically investigated in a silicon nitride waveguide. It is found that the SOD and TOD can affect the frequency shift and temporal profiles of idler pulses. Moreover, the temporal and frequency spectrum of output signal are also discussed with different SODs and TODs. Meanwhile, the numerical simulation results imply that the efficiency of FWM process will be reduced and the wavelength range of phase-match will be shifted due to the change of SOD or TOD.

Keywords: Second-order dispersion; third-order dispersion; wavelength conversion; waveguide.

1. Introduction

In recent years, although the nonlinear silicon photonics for near-IR applications are well known and keep attracting great attention,[1–3] there are some studies about nonlinear silicon photonic, which have been extended to the operating wavelength at mid-infrared region (mid-IR) range. And increasingly researchers pay attention to nonlinear silicon photonics field focusing on mid-IR range, such as optical

frequency comb,[4,5] environment monitoring[6] and optical communication.[7,8] Silicon nitride is an excellent material candidate for nonlinear optics for its transparent and low loss in mid-IR.[9,10] Moreover, its complementary-symmetry metal-oxide semiconductor (CMOS) compatibility makes it more attractive. Silicon nitride has widely been used for optical waveguide,[11] optical switch[12] and optical modulator[13] in the past decade. What is more, silicon nitride exhibits relatively large nonlinear Kerr coefficient ($n_2 = 2.6 \times 10^{-19}$ m^2 W^{-1}), which plays an important role in nonlinear parametric processes.[14] For nonlinear optics field, wavelength conversion has always been a research hotspot for its wide application prospect of signal processing,[15] data transmission,[16] communication[17] and so on. To explore wavelength conversion based on nonlinear effects, comparing with sum-frequency or differential-frequency generation, cross-phase modulation, four wave-mixing (FWM) is the most popular method for the reason that it can be applied to most materials and achieve a large temporal aperture.[18] As is well known, dispersion plays a significant role in FWM process.[19,20] Dispersion is close connection to the efficiency of nonlinear effects due to the relation between phase-match and dispersion. The phase-match among the interacting waves is required in the FWM process, and the phase mismatch is defined as $\Delta k = \Delta\beta + 2\gamma_p p_p$, where $\Delta\beta = k_s + k_i - 2k_p$ is the linear part of the phase mismatch, and k_p, k_s and k_i represent the propagation constants of the pump, signal and idler waves, respectively. The second term is the nonlinear part, where γ_p is the effective nonlinearity of the waveguide, and p_p is the pump power. However, efficient FWM is just able to be reached when the phase-matching condition is satisfied as the relation $\Delta K = 0$.[21] Thus, the impacts of dispersion on FWM are extremely worthy to be investigated, which can help researchers obtain a clearer and deeper understanding about nonlinear parametric processes.

In this paper, we propose a strip silicon waveguide, which can be used for nonlinear parametric processes at mid-IR range. The impacts of SOD and TOD on spectral properties of wavelength conversion are investigated by numerical simulation. According to the results, we can conclude that frequency profile of output signal is shifted and the conversion efficiency of FWM is obviously different with the slight change of SOD or TOD. These results exhibit significant potential applications in nonlinear optics, integrated optics and optical communications.

2. Principle and Device Design

The mature CMOS technology and the development of nanoscale fabrication platforms bring a spring to photonic integration in past several years.[22–24] For example, silicon-on-insulator waveguides have been widely used in devices for its design flexibility, which can take the form of channel waveguides,[25] ridge waveguides,[26] photonic crystal waveguides[27] or slot waveguides.[28] They have been applied to the optical switch,[29] array waveguide grating[30] and optical modulator.[13] In this work, we propose a silicon nitride strip waveguide, which can work in mid-IR range for nonlinear parametric processes. Silicon nitride is deposited on the top of substrate as

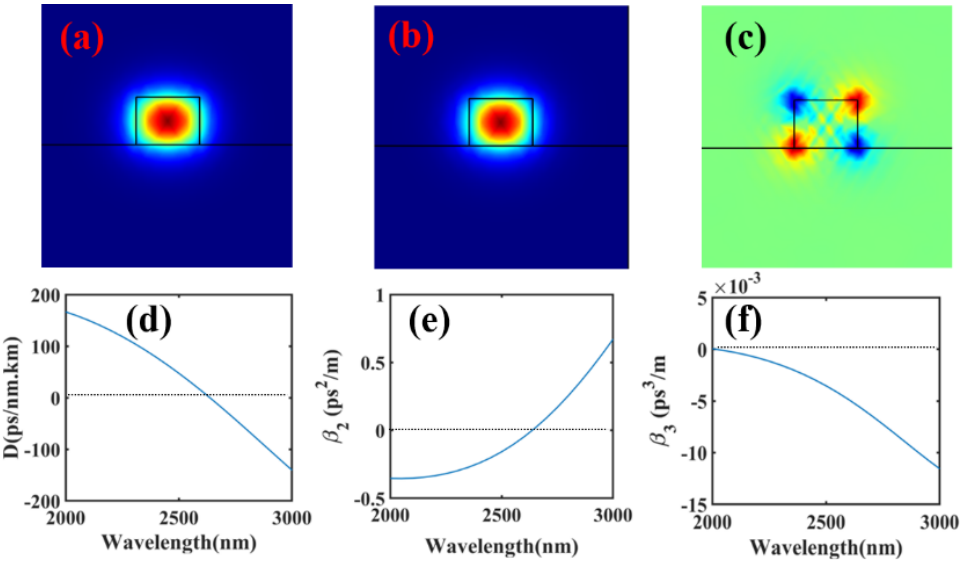

Fig. 1. (Color online) (a) TM mode for the waveguide and (b) E_x and (c) E_y electric field components of the waveguide at the wavelength of 2500 nm, (d) the dispersion and (e) second-order dispersion and (f) third-order dispersion.

silica, the width and height of silicon nitride are set as $w = 1.6$ μm and $h = 1.2$ μm, respectively. When we do numerical simulation by the finite element method, the cladding is set as air. Figures 1(a)–1(c) present the TM mode and E_x and E_y electric field components of the waveguide at the wavelength of 2500 nm, respectively. As we can see from the picture, the most power is restricted in the core material (silicon nitride) and the mode is standard single mode, which imply that the design exhibits good performance. Figures 1(d)–1(f) present the dispersion, second-order dispersion (SOD) and third-order dispersion (TOD), respectively. As mentioned in Sec. 1, the efficient FWM only occurs when phase-match condition is realized. So the second-order dispersion should be minus. According to the simulation results, this waveguide exhibits an effective bandwidth of 500 nm in mid-IR. Moreover, the value of SOD and TOD is smaller than regular waveguides, which contributes to a low threshold system.

3. Simulation and Results

Here, we focus on the degenerate FWM to theoretically investigate wavelength conversion at mid-IR range and explore the influences of SOD and TOD on wavelength conversion, which involves two pump photons at frequency ω_p passing their energy to a signal wave at angular frequency ω_s and an idler wave at angular frequency ω_i as the relation $2\omega_p = \omega_s + \omega_i$ holds.[14] In first condition, we ignore the SOD and TOD and assume the working wavelength focusing on ideal zero-dispersion wavelength. Figures 2(a) and 2(d) present the temporal waveform and frequency

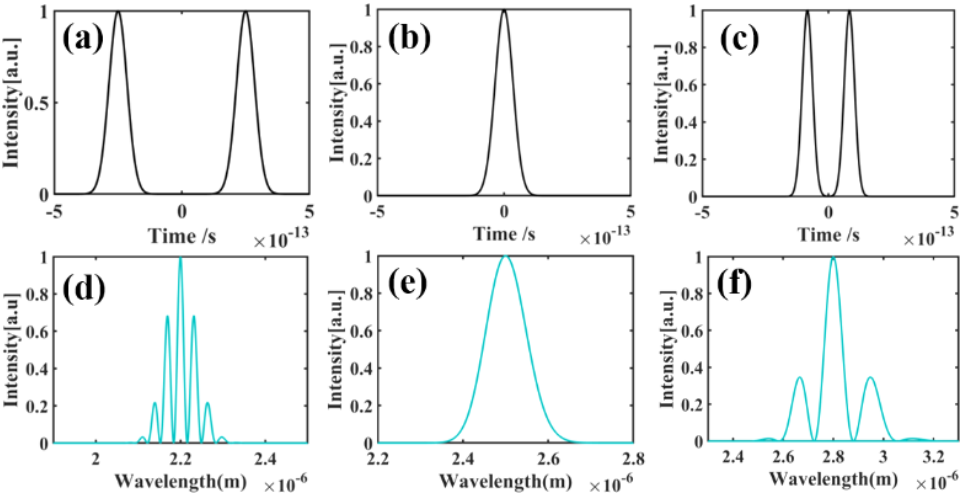

Fig. 2. (Color online) (a) Temporal waveform and (d) frequency spectrum of the input signal, (b) temporal waveform and (e) frequency spectrum of the pump, (c) temporal waveform and (f) frequency spectrum of the output signal.

spectrum of input signal, respectively. It is a signal consisting of two 120 fs-wide pulses separated by 500 fs and the central wavelength is 2200 nm. Figures 2(b) and 2(e) present the temporal waveform and frequency spectrum of pump, respectively. It is a 100 fs pulse of central wavelength at 2500 nm. After the FWM process, the output signal is shown in Figs. 2(c) and 2(f). The central wavelength of output is focused on 2800 nm. The simulation results we can see from Figs. 2(c) and 2(f) are based on ideal condition without taking SOD and TOD into account. Thus, it is able to be a standard reference. When the factor of SOD or TOD is considered in simulation, there is a stark contrast between the results and this reference, which will contribute to analysis of the influences of SOD and TOD on wavelength conversion.

In second condition, the factor of SOD is considered and the simulation results under different values are shown in Fig. 3. Temporal waveform and frequency spectrum of the output signal with considering SOD at 1 ps^2/m are shown in Figs. 3(a) and 3(c), respectively. Temporal waveform and frequency spectrum of the output signal with considering SOD at 0.1 ps^2/m are shown in Fig. 3(b) and 3(d), respectively. Comparing with the standard reference, the temporal spectrum is obviously broaden. The temporal spectrums are totally different under different SOD values. On the other hand, the frequency profile of output signal is changed and the peak is shifted.

In third condition, we simulate the conversion wavelength under three different SOD values with small difference $(1, 2, 3\ ps^2/m)$. As shown in Fig. 4, the green line is the result of 1 ps^2/m, the red line is the result of 2 ps^2/m and the blue line is the result of 3 ps^2/m. According to the results, different SOD means different

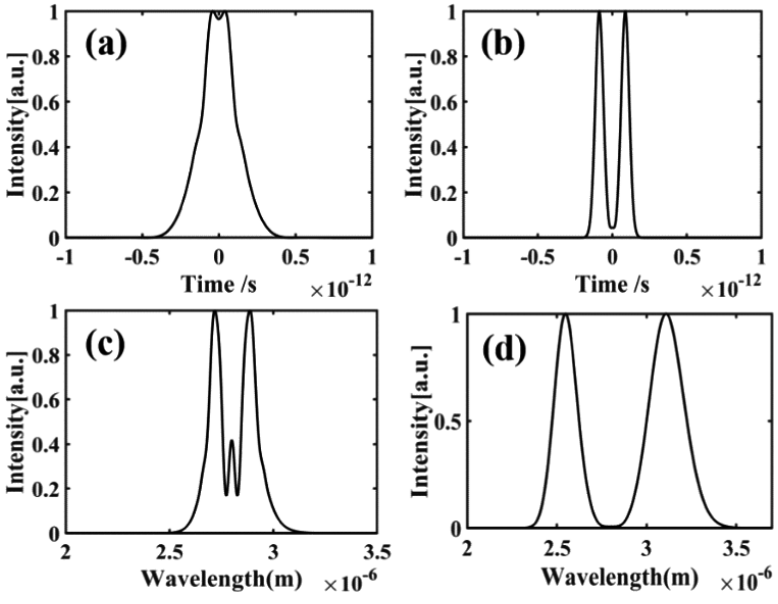

Fig. 3. (a) Temporal waveform and (c) frequency spectrum of the output signal with considering SOD at 1 ps^2/m, (b) temporal waveform and (d) frequency spectrum of the output signal with considering SOD at 0.1 ps^2/m.

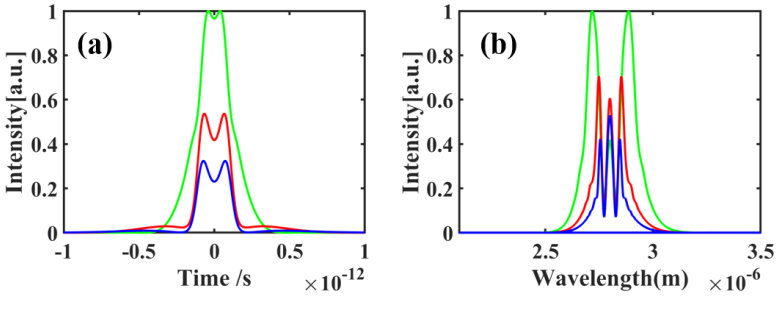

Fig. 4. (Color online) (a) Temporal waveform and (b) frequency spectrum of the output signal with considering different SOD values.

conversion efficiency of power and the bigger SOD means larger loss. When the SOD values are kept in a small difference, the frequency spectrum of output signal will keep similar shape and the central wavelength of output will not shift. If the difference of SOD value is relatively big, the phenomenon will be changed like the results shown in Fig. 3.

In this section, the factor of TOD is taking into account, Figs. 5(a) and 5(c) present the temporal waveform and frequency spectrum of the output signal with considering TOD at 1 ps^3/m, respectively. Figures 5(b) and 5(d) present the temporal waveform and frequency spectrum of the output signal with considering TOD at

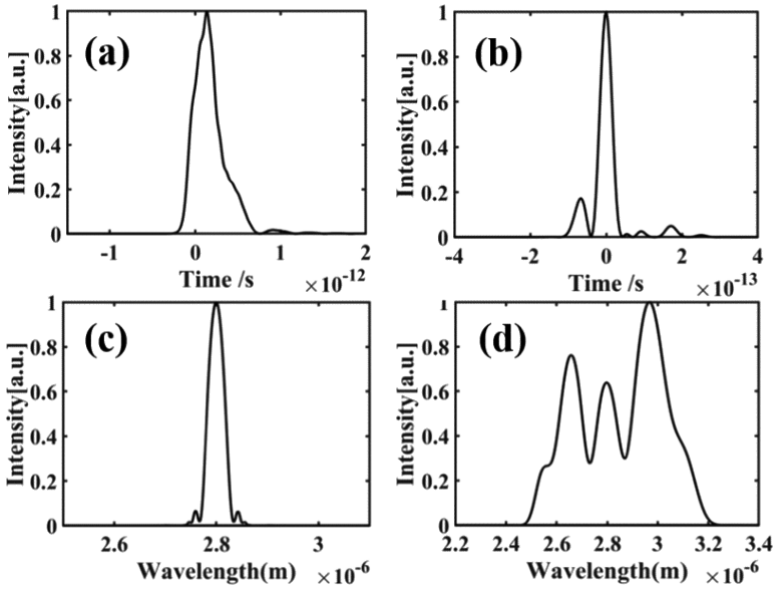

Fig. 5. (a) Temporal waveform and (c) frequency spectrum of the output signal with considering TOD at 1 ps^3/m, (b) temporal waveform and (d) frequency spectrum of the output signal with considering TOD at 0.01 ps^3/m.

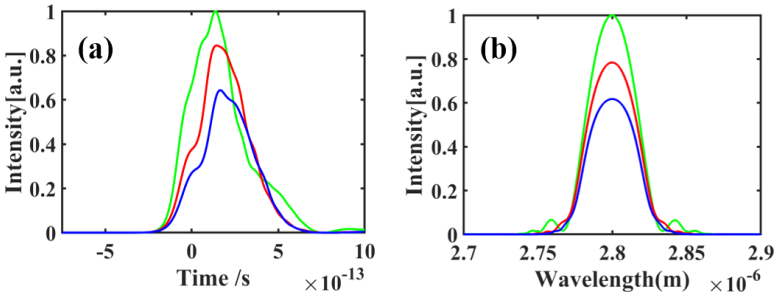

Fig. 6. (Color online) (a) Temporal waveform and (b) frequency spectrum of the output signal with considering different SOD values.

0.01 ps^3/m, respectively. Comparison to SOD, TOD brings a more obvious change on temporal waveform. When a small TOD is considered, the pulse width will not change too heavily, but the new peak will be produced. When the TOD is reach to level of ps^3/m, the width will be broaden. Different TOD means different ranges of idler frequency.

As we can conclude that the bigger TOD will make the frequency profile reduced, but the different TOD will not change the central wavelength of idler frequency. Furthermore, we simulate the conversion wavelength under three different TOD values with small difference $(1, 2, 3\ ps^3/m)$.

As shown in Fig. 6, the green line is the result of 1 ps^3/m, the red line is the result of 2 ps^3/m and the blue line is the result of 3 ps^3/m. Similar to the results of considering SOD, different TOD means different conversion efficiency of power and the bigger TOD causes larger loss. When the TOD values are kept in a small difference, the frequency spectrum of output signal will keep similar shape and the central wavelength of output will not shift. If the difference of TOD value is relatively big, the results will be changed like the results shown in Fig. 5. Thus, considering about the influences of SOD and TOD, we conclude that a flat dispersion waveguide is extremely important to nonlinear parametric processes. It contributes to a low threshold, low loss and stable device, which is a critical spot of future photonic integration system.

4. Conclusion

In this work, the influences of SOD and TOD on wavelength conversion are investigated in detail by solving the coupled mode equations, respectively. It is found that SOD and TOD exhibit the impacts of broadening the temporal profile and making idler frequency shift. Meanwhile, the conversion efficiency will be reduced due to SOD and TOD. According to the phenomenon, it concludes that the most direct way to improve the performance of system depends on optimal devices. We are able to keep the zero wavelength of SOD and TOD around the working wavelength by choosing suitable materials and adjusting the structure of devices, which will efficiently decrease the negative impacts and make it in an acceptable level. These results exhibits wide applications in signal processing, photonic integration and help to a deeper insight of researchers' understanding of the physical mechanisms and nonlinear effects about the optical pulse generation processes.

Acknowledgment

This work was supported by the Strategic Priority Research Program of the Chinese Academy of Sciences (Grant No. XDB24030600) and China Scholarship Council.

References

1. M. Straub and M. Gu, *Opt. Lett.* **27** (2002) 1082.
2. S. Das, A. Salandrino, J. Z. Wu and R. Q. Hui, *Opt. Lett.* **40** (2015) 1516.
3. X. M. Wang, Z. Z. Cheng, K. Xu, H. K. Tsang and J. B. Xu, *Nat. Photonics* **7** (2013) 888.
4. E. Sorokin, A. Marandi, P. G. Schunemann, M. M. Fejer, R. L. Byer and I. T. Sorokina, *Opt. Express* **26** (2018) 9963.
5. H. R. Guo, C. Herkommer, A. Billat, D. Grassani, C. K. Zhang, M. H. Pfeiffer, W. Weng, C. S. Brès and T. J. Kippenberg, *Nat. Photonics* **12** (2018) 330.
6. L. Dong, F. K. Tittel, C. G. Li, N. P. Sanchez, H. P. Wu, C. T. Zheng, Y. J. Yu, A. Sampaolo and R. J. Griffin, *Opt. Express* **24** (2016) 528.
7. G. Z. Mashanovich, F. Y. Gardes, D. J. Thomson, Y. F. Hu and K. Li, *IEEE J. Quantum Elect.* **21** (2015) 8200112.

8. C. Lin, R. Grassi, T. Low and A. S. Helmy, *Nano Lett.* **16** (2016) 1683.
9. P. T. Lin, V. Singh, L. Kimerling and A. M. Agarwal, *Appl. Phys. Lett.* **102** (2013) 251121.
10. P. T. Lin, V. Singh, H. Y. Lin, T. Tiwald, L. C. Kimerling and A. M. Agarwal, *Adv. Opt. Mater.* **1** (2013) 732.
11. A. Z. Subramanian, E. Ryckeboer, A. Dhaka, F. Peyskens, A. Malik *et al.*, *Photonics Res.* **3** (2015) B47.
12. M. A. Vancamp, S. Assefa, D. M. Gill, T. Barwicz, S. M. Shank, P. M. Rice, T. Topuria and M. J. Green, *Opt. Express* **20** (2012) 28010.
13. K. Alexander, J. P. George, J. Verbist, K. Neyts, B. Kuyken, D. V. Thourhout and J. Beeckman, *Nat. Commun.* **9** (2018) 3444.
14. P. Xie, Y. Wen, Z. S. Wan, X. Y. Wang, J. R. Liu, W. Q. Yang, X. F. Li and Y. S. Wang, *Jpn. J. Appl. Phys.* **58**(5) (2019), doi:10.7567/1347-4065/ab0c52.
15. Y. F. Song, Y. X. Chen, X. T. Jiang, W. Y. Liang, K. Wang, Z. M. Liang, Y. Q. Ge, F. Zhang, L. M. Wu, J. L. Zheng, J. H. Ji and H. Zhang, *Adv. Opt. Mater.* **6** (2018) 1701287.
16. H. Hu *et al.*, *Nat. Photonics* **12** (2018) 469.
17. R. Ikuta, T. Kobayashi, T. Kawakami, S. Miki, M. Yabuno, T. Yamashita, H. Terai, M. Koashi, T. Mukai, T. Yamamoto and N. Imoto, *Nat. Commun.* **9** (2018) 1997.
18. P. Xie, Q. Sun, L. Wang, Y. Wen, X. Wang, G. Wang, C. Zeng, M. Liu, Z. Ge and Z. Lu, *Appl. Phys. Express* **11** (2018) 082204.
19. P. Xie, M. T. Xue, Y. Wen, X. F. Li, X. Y. Wang, H. Y. Yin, C. Z. Du, J. R. Liu and J. H. Liu, *Mod. Phys. Lett. B* **10** (2019) 1950053.
20. M. R. Karim, B. M. A. Rahman and G. P. Agrawal, *Opt. Express* **23** (2015) 6903.
21. L. An, H. Liu, Q. Sun, N. Huang and Z. Wang, *Appl. Optics* **53** (2014) 4886.
22. J. F. Bauters, M. L. Davenport, M. J. R. Heck, J. K. Doylend, A. Chen, A. W. Fang and J. E. Bowers, *Opt. Express* **21** (2013) 544.
23. E. Kuramochi, K. Nozaki, A. Shinya, K. Takeda, T. Sato, S. Matsuo, H. Taniyama, H. Sumikura and M. Notomi, *Nat. Photonics* **8** (2014) 474.
24. Z. Shao, Y. J. Chen, H. Chen, Y. Zhang, F. Zhang, J. Jian, Z. Fan, L. Liu, C. C. Yang, L. D. Zhou and S. Yu, *Opt. Express* **24** (2016) 1865.
25. A. Dhaka, A. Raza, F. Peyskens, A. Z. Subramanian, S. Clemmen, N. L. Thomas and R. Baets, *Opt. Express* **23** (2015) 27391.
26. D. Dai, Y. Tang and J. E. Bowers, *Opt. Express* **20** (2012) 13425.
27. S. P. Yu, J. D. Hood, J. A. Muniz, M. J. Martin, R. Norte, C.-L. Hung, S. M. Meenehan, J. D. Cohen, O. Painter and H. J. Kimble, *Appl. Phys. Lett.* **104** (2014) 111103.
28. Z. L. Lu, W. S. Zhao and K. F. Shi, *IEEE Photonics* **4** (2012) 735.
29. L. Chen and Y. K. Chen, *Opt. Express* **20** (2012) 18977.
30. A. Malik, M. Muneeb, S. Pathak, Y. Shimura, J. Van Campenhout, R. Loo and G. Roelkens, *IEEE Photonics Tech. Lett.* **25**(18) (2013) 1805.